AD-A066 318 FOREIGN TECHNOLOGY DIV WRIGHT-PATTERSON AFB OHIO F/G 20/4
EFFECT OF ACOUSTICAL DISTURBANCES ON THE LAMINAR-TURBULENT BOUN--ETC(U)
FEB 78 E V VLASOV, A S GINEVSKIY
UNCLASSIFIED FTD-ID(RS)T-2231-77 NL

| OF |
ADA
066318

END
DATE
FILMED
5-79
DDC

FTD-ID(RS)T-2231-77

①

FOREIGN TECHNOLOGY DIVISION

EFFECT OF ACOUSTICAL DISTRUBANCES ON THE LAMINAR-TURBULENT BOUNDARY LAYER TRANSITION

by

E. V. Vlasov and A. S. Ginevskiy

EDITED TRANSLATION

FTD-ID(RS)T-2231-77 1 February 1978

MICROFICHE NR: FTD-78-C-000158

EFFECT OF ACOUSTICAL DISTURBANCES ON THE LAMINAR-TURBULENT BOUNDARY LAYER TRANSITION

By: E. V. Vlasov and A. S. Ginevskiy

English pages: 19

Source: Uchenyye Zapiski Tsagi, Vol. 2, No. 2,
1971, pp. 1-10.

Country of origin: USSR
Translated by: SCITRAN
F33657-76-D-0390
Requester: AEDC/XRF
Approved for public release; distribution unlimited.

PREPARED BY:

TRANSLATION DIVISION
FOREIGN TECHNOLOGY DIVISION
WP-AFB, OHIO.

Uchenye Zapiski TsAGI vol. 2 , No. 2, pp. 1-10, 1971 RDV

UDC 532.526.011.6:534.2

EFFECT OF ACOUSTICAL DISTURBANCES ON THE LAMINAR-TURBULENT BOUNDARY LAYER TRANSITION

E. V. Vlasov and A. S. Ginevskiy

Results of an experimental investigation into the effect of sound vibrations of different intensity and frequency propagating streamwise on freestream turbulence and on the boundary layer transition are presented. It is shown that the degree of turbulence of longitudinal velocity fluctuations increases abruptly at reasonably high sound intensities, while the degree of turbulence of transverse components of those velocity fluctuations remains virtually unaffected. It is reported that the mechanism underlying a transition induced by sound vibrations may be twofold: the transition is triggered by resonant phenomena in the case of a comparatively weak signal and fully specified frequencies, i.e., by coupling of sound waves and Tolmien-Schlichting waves in the boundary layer.

The study of the effect of noise of different intensity and frequency on the laminar-turbulent boundary layer transition is of great scientific and practical interest. Earlier research [1-5] has uncovered some features of this influence. For instance, Spangler and Wells [2] demonstrated that the transition depends substantially on energy and on the spectrum of acoustical disturbances present. The effect exerted by acoustical disturbances on the transition becomes particularly conspicuous at low initial freestream turbulence. Wells earlier [1] pointed out that maximum critical Reynolds numbers $Re_x = 4.9 \cdot 10^6$ at freestream turbulence $\varepsilon < 0.1\%$. In their classical study, Schubauer and Skramstad [6] found the maximum critical Reynolds number to attain $Re_x = 2.8 \cdot 10^6$ at the same level of turbulence. As pointed out in [2], the low values reported for the critical Reynolds number in the low freestream turbulence Schubauer-Skramstad experiments were caused by acoustical disturbances (wind tunnel blower noise and power plant noise), which constitute an appreciable source of velocity fluctuations (when $\varepsilon < 0.05\%$, about 90% of the total energy associated with the disturbances over the entire spectrum is accounted for by fluctuations of an acoustical nature).

Some interesting conclusions on the effect of sound of different intensity and frequency on the transition in the case of artificial laminarization of the boundary layer by suction were reported by Bacon et al. [3], who made a study of sound propagation both streamwise and athwart the stream.

Knapp and Roache [4] investigated successive stages of both natural and sound-induced onset of boundary layer transition. They conducted their study using a hot-wire anemometer and high-speed motion picture photography of smoke streaks. They reported an upstream shift of the transition region when the sound frequency is close to the frequency of the Tolmien-Schlichting waves, with a drastic change in transition pattern resulting. Their inferences are mainly qualitative. Finally, Schilz [5] has made a study of the effect of sound emission on flow near the stagnation point at the leading edge of a plate swept by longitudinal flow; here the sound propagates at right angles to the stream. It turns out that in this instance both the onset and the suppression of turbulence may be functions of Reynolds number, i.e., sound disturbances of this type could have the effect of either accelerating or, on the contrary, delaying, the transition. The same pattern of ambiguous effects of sound disturbances on the propagation pattern of submerged flows has been reported by the present authors [7] and subsequently confirmed in other studies.

The purpose of this article is to report an investigation of the effect of sound vibrations of different intensity and frequency, propagating streamwise, on freestream turbulence and on the boundary layer transition.

Experimental layout and procedure. The experiments were staged in a wind tunnel at flow velocities not exceeding 25 m/sec. A nonreturn square cross section (100 X 100 mm) wind tunnel with closed working section, tunnel overall length 950 mm, was employed. Air was drawn into the tunnel by a blower, passed through the honeycombed and screened inlet effuser, and through a 25:1 contraction ratio nozzle into the working section. The acoustic field was established by a dynamic loudspeaker, with diffuser placed upstream of the inlet effuser. The acoustical power output of the dynamic loudspeaker was approximately

0.5 W when a pure tone of frequency f = 1000 Hz was broadcast. A pure tone generator or white noise generator served as source for the signal impressed on the dynamic loudspeaker. Bandpass filters with constant relative bandwidth of 1/3 and 1 octave were also employed. The loudspeaker and diffuser were positioned at a distance from the inlet effuser such that the velocity field and turbulence intensity in the inlet end of the working section would experience the least possible distortion.

The mean velocities and three components of the fluctuation velocity were measured with the aid of a hot-wire anemometer set fabricated by Diesa Elektronik . A 1/3 octave Brüll and Kjaer spectrum analyzer was employed in the spectral analysis. The data were then converted to 1 Hz bandwidth. With no stream flowing through the tunnel, a type 4135 Brüll and Kjaer dynamic loudspeaker was used to measure the acoustical pressure in the direction of and at right angles to the tunnel working section. Subsequently, the sound intensity in the tunnel working section was checked for constant level by measuring the voltage across the dynamic loudspeaker with the latter held fixed relative to the inlet effuser. The flow velocity in the tunnel was checked for constant value CONTROL and rarefaction in the working section entrance cross section was kept constant.

A polished wooden flat plate 10 mm thick with rounded leading edge (ellipse with semiaxis ratio 5:1) and span of 100 mm was set up in the tunnel working section 60 mm from the tunnel outer wall. The plane of the plate was lined up parallel to the stream flow direction, while the ends of the plate were set in the side walls of the tunnel working section. The plate surface was reasonably smooth: maximum surface asperities were not in excess of 2 μ, as measured with a profilograph. The plate was vented, with holes spaced 25 to 50 mm apart on the top surface at a distance of 10 mm from the plate center, while venting connections led out below allowing the pressure to be transmitted via rubber tubing to a multicontact switch and further on to a micromanometer. Measurements of the pressure distribution over the plate revealed a slight negative longitudinal pressure gradient due to boundary layer buildup on the plate itself and on the walls of the tunnel working section [$d\bar{p}/dx$ = --0.3 per

p3 meter, $\bar{p} = (p - p_\infty)/\frac{1}{2}\rho V_\infty^2$].

A lengthwise slit covered by a sliding bar was cut in the top wall of the tunnel working section. This made it possible to use Pitot microprobes or a single-filament hot-wire attachment to measure total pressure or the longitudinal component of velocity fluctuations along the plate at a fixed distance from the surface. The distance was set with the aid of a spring-loaded device. These measurements were then used to locate the transition region in the boundary layer on the flat plate. Traversing microprobes positioned on the sliding bar, and airflow metering and hot-wire attachments, were also used to measure the mean velocity and turbulence intensity inside and outside the boundary layer. Control measurements were taken in the boundary layer over the plate span (at a distance of ± 25 mm from the symmetry plane), showing that the layer can be treated safely as two-dimensional at distances of up to 300 mm from the plate leading edge.

Preston tubes were employed to measure the local surface friction coefficient. The configuration of the transition zone on the plate was found from the rate of evaporation of methyl alcohol applied to the kaolin coating on the plate.

Measurements of the distribution of sound pressure levels along the working section axis while the dynamic loudspeaker was emitting pure tones, sounds in 1/3-octave and full-octave bands, and white noise, showed a decrease in the nonuniformity of sound intensity along the duct as the range of frequencies of sound emitted was expanded. Nonuniformity of the sound energy distribution in various cross sections through the tunnel working section did not exceed 3-5 dB in the case of a pure tone or 1-2 dB in the case of sound emitted in the octave frequency bands.

The effect exerted by the acoustical disturbances on isotropic turbulence. The primary focus here is on investigation of the effects of sound vibrations on stream turbulence outside the boundary layer. Below we consider some basic findings resulting from this study.

Measurements of the turbulence intensity of three fluctuation velocity components and of the corresponding spectra in the absence of sound disturbances revealed that these characteristics remain practically unaltered in the streamwise direction. Figure 1 shows spectra of the three components of the fluctuation velocity at the same distance from the working section inlet end. Here we see that the turbulence intensities of all three components of the pulsation velocity, the longitudinal component u' and the two transverse components v' and w', are practically identical, viz. $\varepsilon_u \approx \varepsilon_v \approx \varepsilon_w \approx 0.3\%$. The values of the one-point correlation coefficients between the longitudinal and one of the two transverse components of the velocity fluctuations were close to zero.

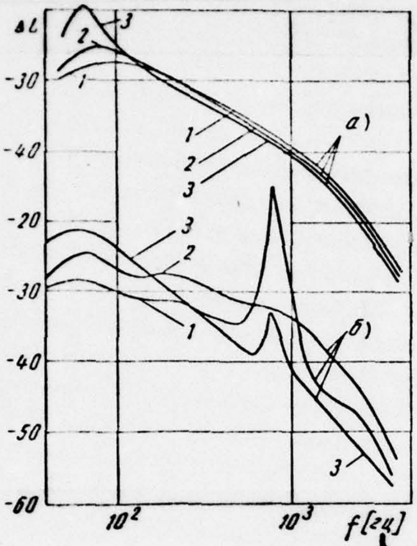

a) sound signal absent:

1) $\Delta L_u = 20 \log (u'_f / u'_\Sigma)$; 2) $\Delta L_v = 20 \log (v'_f / u'_\Sigma)$;

3) $\Delta L_w = 20 \log (w'_f / u'_\Sigma)$, where u'_f, v'_f, w'_f are the rms velocity fluctuations at frequency f ; u'_Σ is the total rms value for the longitudinal fluctuations;

b) for L = 130 dB, f = 800 Hz:

1) $\Delta L_u = 20 \log (u'_f / u'_{\Sigma 0})$; 2) $\Delta L_v = 20 \log (v'_f / u'_{\Sigma 0})$;

3) $\Delta L_w = 20 \log (w'_f / u'_{\Sigma 0})$, where $u'_{\Sigma 0}$ is the total rms value for the longitudinal fluctuations with sound signal absent.

Fig. 1. Spectra of velocity fluctuations in free stream at flow velocity V_∞ = 15 m/sec; x = 370 mm.

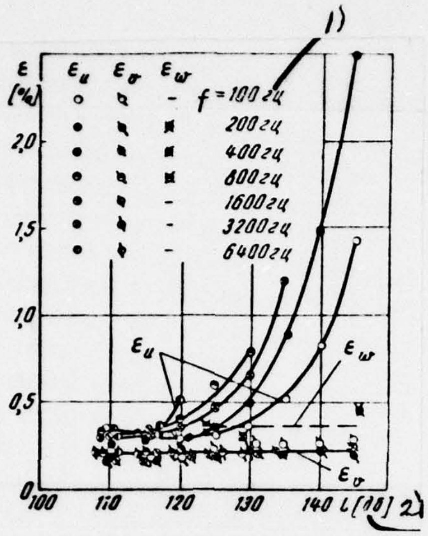

Fig. 2. Effect of intensity and of frequency of sound on degree of turbulence of three components of the fluctuation velocity in free stream, at $V_\infty = 15$ m/sec and x = 327 mm.

1) Hz 2) dB

The agreement between values for the intensity of turbulence of the three velocity fluctuation components, the agreement between their spectra, and the zero value of the single-point correlation coefficients over the entire tunnel working section, all argue for a virtually isotropic and uniform turbulence throughout the working section of the wind tunnel.

When sound vibrations of sufficiently great intensity propagate downstream, the turbulence intensity of the longitudinal component of the velocity increases abruptly, while the turbulence intensity of the two transverse components of the fluctuation velocity remain practically unaffected (Fig. 2).

Results of a spectral analysis (see bottom curves in Fig. 1) also reveal that superposition of a sound signal of specified frequency brings about an increase in the longitudinal component of the velocity fluctuations at precisely that frequency (or one of its harmonics) while affecting the transverse components of the velocity fluctuations to a far lesser extent. When the sound signal level is appreciably high, the total turbulence intensity of the longitudinal component of the velocity fluctuations is determined completely by the velocity fluctuations at the frequency of the superposed signal. As flow velocity is increased, the effect of the sound disturbances on the longitudinal component of the velocity fluctuations slackens off, while ε_u decreases in inverse proportion to the flow velocity. We see then that the fluctuations in velocity are generated by the sound disturbances in the form of a plane wave.

The isotropic turbulence is rendered initially nonisotropic by the effect of the sound vibrations propagating downstream; the degree of turbulence ε_u undergoes a steep increase at fairly high sound intensities, while the turbulence pattern remains virtually unaltered over a stretch of 500 mm in the streamwise direction.

Effect of acoustical disturbances on the characteristics of the laminar boundary layer and on the laminar-turbulent transition. The transition region in the plane of symmetry of the flat plate is situated within the tunnel working section at a distance of 300 to 500 mm from the leading edge of the plate. This is illustrated in Fig. 3a by the dependences of the intensity of fluctuations in the longitudinal component of the velocity at a fixed distance $y_0 = 0.3$ mm from the plate surface, as a function of the longitudinal coordinate and of the flow velocity in the absence of sound disturbances. These relationships allow us to determine the origin and extent of the transition region. For example, at velocity $V_\infty = 15$ m/sec, the onset of transition occurs at roughly $x \approx 300$ mm and transition terminates at $x \approx 400$ to 500 mm, which corresponds to a critical Reynolds number $Re_x = V_\infty x/\nu \approx 0.4 \cdot 10^6$. The fact that the value of the critical Reynolds number (at freestream turbulence 0.3%) is on the low side is attributed to end effects, viz., closure of turbulent wedges formed at sites where the plate leading edge abuts the tunnel sidewalls. Further evidence of this is provided in particular by a photograph of the transition process obtained via the kaolin coating method (see Fig. 3d).

Profiles of mean velocity and longitudinal component of the fluctuation velocity in the boundary layer are plotted in Fig. 4. The change experienced by these profiles is in satisfactory agreement with the boundaries of the transition region indicated in Fig. 3. Boundary wall thicknesses, specifically the displacement thickness δ^*, the momentum loss thickness δ^{**}, and the ratio of the two $H = \delta^*/\delta^{**}$, were calculated on the basis of the velocity profiles so measured.

We find from the results that the ratio H decreases with increasing distance from the plate leading edge: near the leading edge we have $H \approx 2,5$, but at the end of the transition interval this ratio becomes $H \approx 1.5$.

Additional information on the characteristics of the boundary layer in the transition region can be gained from examination of the spectra of fluctuations in longitudinal stream velocity near the plate surface and in free stream. These spectra diverge negligibly in the

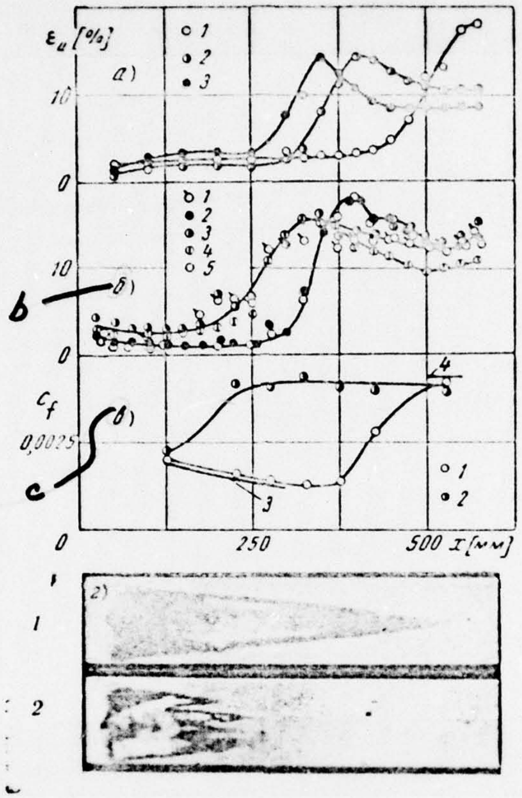

Figure 3

(See following page for caption.)

a) variation in intensity of longitudinal velocity fluctuations along axis at fixed distance from plate surface y_c = 0.3 mm with sound signal absent: 1) V_∞ = 7.5 m/sec; 2) $V_{\%}$
2) V_∞ = 15 m/sec; 3) V_∞ = 24 m/sec
b) with sound present: 1) L = 130 dB and f_{av} = 800 Hz;
2) L = 130 dB and f_{av} = 200 Hz; 3) L = 140 dB and f_{av} = 200 Hz;
4) white noise, L = 126 dB; 5) sound signal absent;
c) effect of acoustical disturbances on local friction coefficient at freestream velocity V_∞ = 15 m/sec:
1) sound signal absent; 2) sound present, of intensity L = 130 dB and frequency f = 800 Hz; 3) theoretically predicted c_f for laminar boundary layer; 4) theoretically predicted c_f for turbulent boundary layer;
d) visualization of transition on flat plate in the absence of sound disturbances (1) and with sound of intensity L = 130 dB and frequency f = 800 Hz present. Velocity V_∞ = 15 m/sec.

p6

Fig. 3. Transition pattern in flow over plate in the presence and absence of sound disturbances

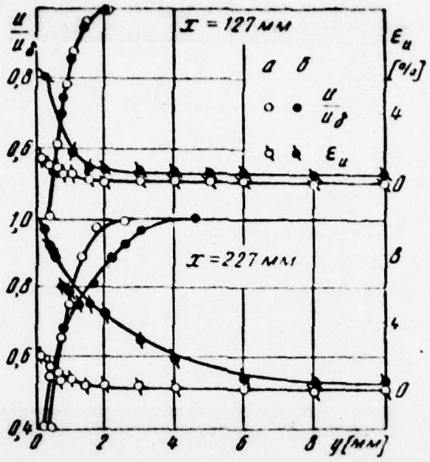

Fig. 4. Profiles of mean velocity and turbulence intensity of the longitudinal component of fluctuation velocity in the boundary layer (V_∞ = 15 m/sec) in the absence of sound disturbances (a) and with sound disturbances of intensity L = 130 dB, frequency f_{av} = 800 Hz in the octave frequency band present (b).

---

laminar boundary layer and in free stream, i.e., velocity fluctuations within the laminar layer are due primarily to stream velocity fluctuations outside the boundary layer. The difference between the spectra for the interior and exterior of the layer emerges quite sharply in the transition region and the region of developed turbulent boundary layer. The variation in the spectra of longitudinal velocity fluctuations at a fixed distance y_0 = 0.3 mm from the plate in the laminar, transitional, and turbulent regions of the boundary layer along the plate is displayed in Fig. 5a.

Curves of the intensity of fluctuations in longitudinal velocity ε_u as a function of x were plotted on the basis of the measurements, for a fixed distance from the surface ($y_0 \approx$ 0.3 mm) in the

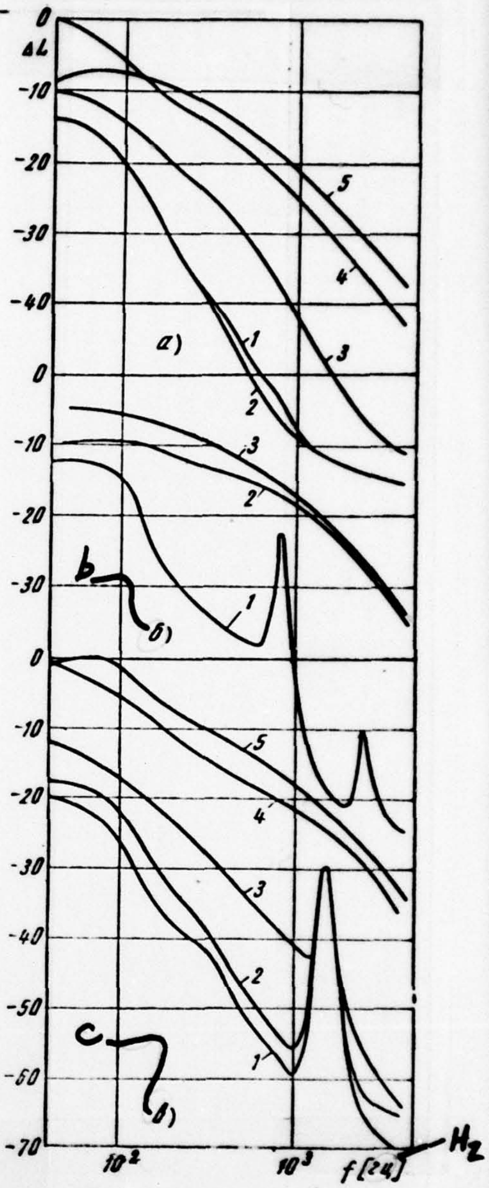

a) no sound signal present:

1) x = 100 mm, = 1.52 %;

2) x = 250 mm, = 2.03 %;

3) x = 300 mm, = 2.96 %;

4) x = 350 mm, = 8.23 %;

5) x = 500 mm, = 11 %;

b) sound signal L = 126 dB, f = 800 Hz;

1) x = 150 mm, = 2.73 %;

2) x = 250 mm, = 8.20 %;

3) x = 400 mm, = 9.07 %;

c) sound signal L = 120 dB, f = 1600 Hz;

1) x = 150 mm, = 1.33 %;

2) x = 250 mm, = 1.76 %;

3) x = 300 mm, = 3.08 %;

4) x = 350 mm, = 9.90 %;

5) x = 400 mm, = 12.30 %.

p7

Fig. 5. Spectra of fluctuations in longitudinal component of velocity at fixed distance y_0 = 0.3 mm from plate (V_∞ = 15 m/sec)

case of a broad range of sound intensity levels L and frequencies f (pure tone, 1/3 octave, full octave) at velocities V_∞ = 7.5 to 24 m/sec, and also for the case where white noise of different intensity levels is involved. Some of these relationships are displayed in Fig. 3*.

We learn from these relationships that sound speeds up the onset of boundary layer transition only under certain sets of conditions. This outcome requires that the sound disturbances be of specified frequency and of sufficiently high intensity. For example, at velocity $V_\infty = 15$ m/sec and L = 110 dB and 115 dB the sound disturbances have no effect on the transition, at L = 120 dB and 125 dB the effect is detected only at frequency f = 800 Hz, at L = 130 dB and 135 dB the effect of sound disturbances on the transition makes itself felt at frequencies f = 200, 400, and 800 Hz, and finally at L = 140 dB the transition is speeded up even at f = 100 Hz.

Here we must take note of two important facts. First, the way sound of specified intensity affects the onset of transition does not depend much on the transmission bandwidth (pure tone, 1/3 octave, or full octave). Second, white noise at L < 120 dB is without effect on the transition. But when a certain sound intensity level is attained, the white noise also brings about an earlier onset of the transition. This result is illustrated in Fig. 3b in the case L = 126 dB.

---

*It should be noted that the maximum intensities of velocity fluctuations, other things being equal, differ slightly in the different series of experiments, because of the nonidentical fixed distances y_o assigned in the different experiments.

Local surface friction coefficients determined with the aid of Preston tubes are also shown in Fig. 3c. The $c_f(x)$ curves are in close agreement with hot-wire anemometer measurements data taken in the transition region, and attest to a conspicuous effect exerted by the sound disturbances on the local surface friction coefficient. As is clear from Fig. 3c, the predicted local surface friction coefficients in purely laminar flow and in turbulent flow fit closely to the corresponding experimentally derived c_f values.

Measurements of profiles of the mean velocity and fluctuation velocity in the boundary layer in the presence of sound disturbance revealed that in those cases where the sound triggered a premature onset of transition appreciable deformation of the profiles of the mean and fluctuation velocity resulted (cf. Fig. 4), with a concomitant change in the integrated characteristics of the boundary layer.

The inferences drawn above found further confirmation in spectral analysis of the longitudinal velocity fluctuations in the boundary layer (Fig. 5b, 5c). These data illustrate the pattern of variation of the spectrum in response to the sound disturbance. In the first case, the effect of a signal of frequency f = 800 Hz and loudness L = 126 dB brings about a rapid boundary layer transition; the frequency of the signal imposed is detected only in the spectrum of the laminar boundary layer. In the second case, a signal of the same intensity, but of doubled frequency, failed to bring about a transition, while the frequency of the signal imposed is viewed in the spectrum of both the laminar boundary layer and the transition boundary layer.

p8

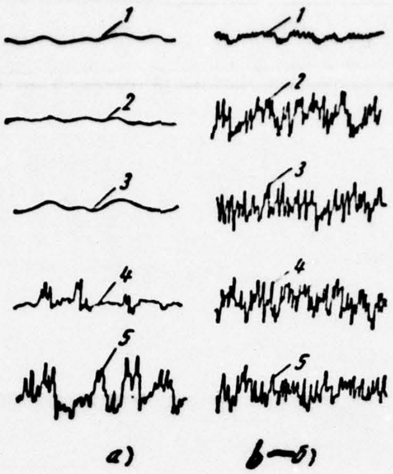

1) $x = 150$ mm, 2) $x \approx 200$ mm, 3) $x = 300$ mm,

4) $x = 360$ mm, 5) $x \approx 400$ mm.

Fig. 6. Oscillograms taken of velocity fluctuations in the boundary layer ($V_\infty \approx 15$ m/sec, $y_0 = 0.3$ mm) in the absence of sound signal, (a), and in the presence of a sound signal such that $L = 126$ dB, $f = 800$ Hz.

Over the range of loudness levels investigated in the present article, the acoustic disturbances not only failed to affect the integrated characteristics of the turbulent boundary layer, but were also without affect on the spectral characteristics of that layer. The reason is that the net energy associated with turbulent fluctuations in the turbulent boundary layer is commensurate with, or even in excess of, the energy associated with fluctuations brought about by the sound signal.

A graphical representation of transition behavior in the absence and presence of sound disturbances is provided by the oscillograms in Fig. 6 showing velocity fluctuations in the boundary layer at $y_0 = 0.3$ mm and at different x .

Special experiments were also staged to investigate the effect of acoustical disturbances on the vertex angle of turbulence wedges forming on a plate downstream of an isolated asperity element or at sites where the plate leading edge abuts the tunnel sidewalls. In those experiments, the transition zone was determined from the pattern of evaporation of methyl alcohol applied to the kaolin coating of the plate. It was found that the vertex angle of the turbulence wedges remained virtually unaffected by acoustical disturbances over the entire sound loudness and frequency ranges investigated. The visually ascertained position of the transition region is in satisfactory agreement with results of hot-wire anemometer measurements. The fact that the vertex angle of lateral turbulence wedges near the end faces of the plate is independent of acoustical disturbances implies that the upstream displacement of the transition region on the symmetry axis that those disturbances cause is not a result of end effects, but is due rather to critical phemomena occurring in the mid-span boundary layer on the plate (Fig. 3d).

It was pointed out earlier that the effect exerted by the acoustic signal tends to increase freestream turbulence. But we cannot jump to the conclusion that the premature onset of boundary layer transition due to the acoustical signal stems solely from the influence of freestream turbulence. In fact, freestream turbulence increases more or less identically at all frequencies of the applied signal as sound intensity is increased, whereas the premature onset of transition takes place only at certain specified frequencies.

The mechanism underlying the transition artificially induced by the acoustical signal may be twofold. First, when the signal is very strong, and when the degree of freestream turbulence increases markedly, the transition may be due precisely to that turbulence, without regard to signal frequency (Taylor scheme). Second, at comparatively low sound signal levels when freestream turbulence is enhanced only negligibly, the transit may be due to resonance phenomena, i.e., to coupling of the applied sound waves and Tolmien-Schlichting waves in the boundary layer.

For a qualitative analysis of this second possibility, we have to turn to hydrodynamic stability theory. It must be stressed, however, that application of this theory runs into difficulties here since the speed of propagation and the wavelength of the sound disturbances diverge markedly from the corresponding parameters of Tolmien-Schlichting waves.

Stability of the laminar boundary layer in the case where the freestream velocity contains a periodic sinusoidally time-varying component of specified amplitude and frequency has been studied in quasisteady state by Pushkareva [8]. The most dangerous frequency range, the one in which the critical Reynolds number takes on its minimum value independently of the amplitude of that periodic component, was delineated. A band corresponding to these dangerous frequencies in Sh, Re* coordinates is found in conformity with

$$\mathrm{Sh}\ \mathrm{Re}^* = \text{const},$$

where the Strouhal and Reynolds numbers are arrived at from the formulas

p 10

$$\mathrm{Sh} = f\delta^*/V_\infty, \quad \mathrm{Re}^* = V_\infty \delta^*/\nu;$$

The results show that, as in the experiments discussed in [3, 4], the range of sound signal frequencies capable of triggering the onset of boundary layer transition at minimum sound intensity corresponds, in a rough approximation, to the instability range of the laminar boundary layer in Sh/Re*, Re* coordinates. The [illegible] boundary layer transition induced by the sound signal also sets in at Sh and Re* values remote from the instability region. In that case the transition is due to enhanced freestream turbulence (ε_u = 2 to 3 %) at sound intensity levels L = 140 to 145 dB.

In conclusion, we note that the forward shift of the transition region in those cases where it is not in and of itself appreciable may exert a substantial effect on the efficiency of artificial laminarization of the boundary layer via discrete suction of air through a slotted surface [3].

The authors take this opportunity to express their thanks to V. M. Filippov for welcome critical remarks.

LITERATURE CITED

1. **Walls** C. S. Effects of freestream turbulence on boundary-layer transition. AIAA J., vol. 5, No 1, 1967.
2. **Spangler** I. G., **Walls** C. S. Effects of freestream disturbances on boundary-layer transition. AIAA J., vol. 6, No 3, 1968.
3. **Bacon** J., **Pfenninger** W., **Moore** C. Investigations of a 30° swept and a 17-foot chord straight suction wing in the presence of internal sound, external sound and mechanical vibrations. Summary of Laminar Boundary Layer Control Research (ASD TDR—63-554), vol. 1, 1964.
4. **Knapp** C. F., **Roache** P. J. A combined visual and hot-wire anemometer investigation of boundary-layer transition. AIAA J., vol. 6, No 1, 1968.
5. **Schilz** W. Experimentelle Untersuchungen zur akustischen Beeinflussung der Strömungsgrenzschicht in Luft. Acustica, vol. 16, No 4, 1965/66.
6. **Schubauer** G. B., **Skramstad** H. K. Laminar boundary-layer oscillations and transition on a flat plate. NASA Techn. Rep., 1948, No 909.
7. **Власов** Е. В., **Гиневский** А. С. Акустическое воздействие на аэродинамические характеристики турбулентной струи. Изв. АН СССР, МЖГ, 1967, № 4.
8. **Пушкарева** И. В. *Ламинарный пограничный слой на плоской пластине в осциллирующем потоке.* ПМТФ, VII—VIII, № 4, 1968.

DISTRIBUTION LIST

DISTRIBUTION DIRECT TO RECIPIENT

ORGANIZATION	MICROFICHE	ORGANIZATION	MICROFICHE
A205 DMATC	1	E053 AF/INAKA	1
A210 DMAAC	2	E017 AF/ RDXTR-W	1
B344 DIA/RDS-3C	8	E404 AEDC	1
C043 USAMIIA	1	E408 AFWL	1
C509 BALLISTIC RES LABS	1	E410 ADTC	1
C510 AIR MOBILITY R&D LAB/FIO	1	E413 ESD	2
		FTD	
C513 PICATINNY ARSENAL	1	CCN	1
C535 AVIATION SYS COMD	1	ETID	3
		NIA/PHS	1
C591 FSTC	5	NICD	5
C619 MIA REDSTONE	1		
D008 NISC	1		
H300 USAICE (USAREUR)	1		
P005 ERDA	1		
P055 CIA/CRS/ADD/SD	1		
NAVORDSTA (50L)	1		
NASA/KSI	1		
AFIT/LD	1		